Journal of Biomolecular NMR, 4 (1994) 201–213
ESCOM

J-Bio NMR 173

Time-saving methods for heteronuclear multidimensional NMR of (^{13}C,^{15}N) doubly labeled proteins

Rolf Boelens*, Maurits Burgering, Rasmus H. Fogh and Robert Kaptein

Bijvoet Center for Biomolecular Research, Department of Chemistry, Utrecht University, Padualaan 8, 3584 CH Utrecht, The Netherlands

Received 20 August 1993
Accepted 28 September 1993

Keywords: Heteronuclear NMR; (^{13}C,^{15}N) triple-resonance NMR; Multidimensional NMR; Proteins

SUMMARY

Heteronuclear 2D (^{13}C,^{1}H) and (^{15}N,^{1}H) correlation spectra of (^{13}C,^{15}N) fully enriched proteins can be acquired simultaneously with virtually no sensitivity loss or increase in artefact levels. Three pulse sequences are described, for 2D 'time-shared' or TS-HSQC, 2D TS-HMQC and 2D TS-HSMQC spectra, respectively. Independent spectral widths can be sampled for both heteronuclei. The sequences can be greatly improved by combining them with field-gradient methods. By applying the sequences to 3D and 4D NMR spectroscopy, considerable time savings can be obtained. The method is demonstrated for the 18 kDa HU protein.

INTRODUCTION

Recent methodological advances in protein NMR have made it possible to study molecules with molecular weights up to 30 kDa (Clore and Gronenborn, 1991; Bax and Grzesiek, 1993). Thus, (^{13}C,^{15}N) isotope double-labeling combined with triple-resonance J-correlation techniques has led to efficient resonance assignment strategies (Ikura et al., 1990a) and all ^{13}C,^{15}N and ^{1}H nuclei of even large proteins can now be assigned in a relatively short time. For structure determination, progress has been made through combination of NOE measurements with heteronuclear multidimensional NMR methods. Three-dimensional ^{15}N- and ^{13}C-separated NOESY experiments resolve ambiguities due to overlap in one proton dimension (Marion et al., 1989; Zuiderweg and Fesik, 1989; Ikura et al., 1990b; Zuiderweg et al., 1990), while 4D HMQC-NOESY-

*To whom correspondence should be addressed.

Abbreviations: HMQC, heteronuclear multiple-quantum coherence spectroscopy; HSQC, heteronuclear single-quantum coherence spectroscopy; HSMQC, heteronuclear single- and multiple-quantum coherence spectroscopy; NOESY, nuclear Overhauser enhancement spectroscopy.

HMQC techniques can do the same in both proton dimensions (Kay et al., 1990; Clore et al., 1991; Zuiderweg et al., 1991). A drawback of the addition of each new dimension is that it always leads to a reduction in resolution for an existing domain, given the same measuring time. Therefore, considerable effort has been undertaken to minimize measuring times by combining phase cycles (Bax et al., 1990a) and by developing gradient techniques for coherence selection and artefact suppression (Hurd, 1990; Vuister et al., 1991; Bax and Pochapsky, 1992; Davis et al., 1992; Keeler et al., 1993; Vuister et al., 1993). Nevertheless, compromises remain between high resolution, multiple dimensions and recording time.

Thus far, most heteronuclear NMR techniques have been based on selection of either ^{13}C- or ^{15}N-attached proton magnetization. Thus, 2D HMQC (Müller, 1979; Bax et al., 1983; Bendall et al., 1983) and HSQC techniques (Bodenhausen and Ruben, 1980; Bax et al., 1990b) exist, which have either a ^{15}N or a ^{13}C t_1-evolution period. Therefore, in order to observe all protons of a (^{13}C,^{15}N) doubly labeled protein two experiments are required. For 3D and 4D NMR, where the HMQC and HSQC sequences are used as building blocks (Clore and Gronenborn, 1991), this implicates that at least two lengthy multidimensional experiments have to be executed. Correlating all protons by HMQC-NOESY-HMQC methods requires even more multidimensional experiments. We will show that the ^{13}C and ^{15}N evolution periods of 2D HMQC and HSQC experiments of (^{13}C,^{15}N) doubly labeled proteins can easily be combined, leading to a high efficiency in measuring time. The time reduction is based on the fact that each proton is bound either to a ^{13}C or to a ^{15}N nucleus so that, since the protons are mainly J-coupled to these nuclei and not further along the backbone, independent coherences can be created for both types of protons. The proposed method is related to a suggestion by Sørensen (1990) that the ^{13}C and ^{15}N evolution for the nuclei attached to these protons could be recorded simultaneously and discriminated afterwards by independent phase cycling and linear combination of the resulting spectra. A first example of such a method was described by Farmer (1991), with the application of a simultaneous (^{13}C,^{15}N)-HMQC on a small peptide. Here we will show that these experiments are feasible for larger proteins, that similar principles can be applied to other heteronuclear correlation experiments and that they can be greatly improved using field-gradient methods. In addition, we will demonstrate that the polarization transfer and the spectral widths of both heteronuclei can be independently optimized and that in most cases the independent phase cycling will not be necessary, which allows a further time saving.

EXPERIMENTAL METHODS

Figures 1A–C show the new 2D time-shared (TS) HMQC, TS-HSQC and TS-HSMQC pulse sequences for (^{13}C,^{15}N) doubly labeled proteins. It can be seen that all three pulse sequences contain the same number of 90° and 180° rf pulses for each nucleus as the conventional separate (^{15}N,^{1}H) and (^{13}C,^{1}H) correlation experiments, but that the pulses for ^{15}N and ^{13}C are applied at different times. The differences are due to the fact that the proton attached to the heteronucleus with the largest $^1J_{HX}$ coupling constant (in this case ^{13}C) needs to be decoupled from the heteronucleus for a period $\delta = (1/2J_{NH} - 1/2J_{CH})$ in order to obtain optimal polarization transfer with both nuclei. We will first describe in product-operator terms (as defined in Ernst et al. (1987)) the flow of magnetization across the new TS-HSQC sequence (Fig. 1A). The convention used will be H, C, and N for proton, carbon and nitrogen magnetization, respectively. We will only consider $^1J_{CH}$

and $^1J_{NH}$ interactions, neglect any potential $^1J_{CC}$ couplings, multiple-bond couplings as well as relaxation effects and consider only terms which will pass the phase cycles. Furthermore, for ease of description we will assume that the delays for polarization transfer, τ_n and τ_c, are chosen exactly as 1/2J, although in case of relaxation smaller values can (and will) be chosen for optimal signal intensity. At time a the magnetization of protons attached to ^{15}N has fully turned into antiphase magnetization, since $\tau_n = 1/(2\ ^1J_{NH})$, i.e., $-2H_xN_z$, while for the protons bound to ^{13}C the magnetization term is antiphase as well, i.e., $-2H_xC_z$, since they were decoupled for a period δ and $^1J_{CH}$ was only effective during a period $\tau_c = 1/(2\ ^1J_{CH})$. At time b the antiphase magnetization $-2H_xN_z$ has turned into $-2H_zN_y$, and the ^{15}N evolution can start for the period t_1^n. For carbon, however, spin order has been generated, i.e., $2H_zC_z$, and this term will remain along the z-axis for a period $(t_1^n - t_1^c)/2$. This allows an independent incrementation of the t_1^n and t_1^c evolution periods. At time c the carbon-attached magnetization is brought into the xy-plane and the resulting antiphase magnetization term, $-2H_zC_y$, can evolve during the time period t_1^c. At times d, e and f the reverse events occur:

$$-2H_zN_y \cos \omega_n t_1^n \xrightarrow{e} 2H_yN_z \cos \omega_n t_1^n \xrightarrow{f} -H_x \cos \omega_n t_1^n$$

$$-2H_zC_y \cos \omega_c t_1^c \xrightarrow{d} -2H_zC_z \cos \omega_c t_1^c \xrightarrow{e} 2H_yC_z \cos \omega_c t_1^c \xrightarrow{f} -H_x \cos \omega_c t_1^c$$

Thus, for each type of proton, magnetization will evolve during t_1 with the frequency of its own attached heteronucleus, in both cases as antiphase magnetization on the heteronucleus as in a regular HSQC spectrum. Since t_1^n and t_1^c can be incremented independently, *two* frequency axes will result, which is favourable since the spectral widths (in Hz) of ^{15}N and ^{13}C can be very different. The independent incrementation demands that the carbon magnetization is deposited for an incrementing time $(t_1^n - t_1^c)$ as H_zC_z spin order, where part of it could be lost due to relaxation. In cases of rapid relaxation this deposition could be avoided, but then an equal spectral width (in Hz) for both nuclei will result.

A very similar approach can be applied to HMQC spectroscopy, as shown in the pulse sequence of Fig. 1B. At time a the multiple-quantum coherence H_xN_y has fully developed, since $\tau_n = 1/(2\ ^1J_{NH})$. During the following t_1^n period this coherence will evolve at a ^{15}N frequency and it will turn into observable magnetization at c as $-H_y \cos \omega_n t_1^n$. This is, of course, not different from a regular 2D HMQC sequence. One approach could be to apply all ^{13}C rf pulses simultaneously with the ^{15}N pulses (Farmer, 1991), but the use of the delay τ_n for ^{13}C-attached protons would result in suboptimal polarization transfer. Therefore, we decouple first for a period $\delta = (\tau_n - \tau_c)$ and in the following period $\tau_c = 1/(2\ ^1J_{CH})$ the proton antiphase term H_xC_z can fully develop. At time b there will be H_xC_y multiple-quantum coherence, which will be observed at c as $-H_y \cos \omega_c t_1^c$. As with the HSQC sequence, the t_1^n and t_1^c evolution periods can be incremented with different values, leading to optimal spectral widths for both nuclei. For this HMQC sequence an independent incrementation can be obtained at the expense of an increase of the ^{13}C decoupling period δ. Since the HMQC sequence contains fewer rf pulses than the HSQC sequence, fewer artefacts due to short phase cycles and less intensity loss due to incomplete flip angles can be expected.

The third pulse scheme (Fig. 1C) shows a so-called HSMQC pulse sequence, a combined HMQC and HSQC sequence, as developed by Zuiderweg (1990). During the t_1 evolution period of the original HSMQC sequence a mixture of single-quantum and multiple-quantum coherences

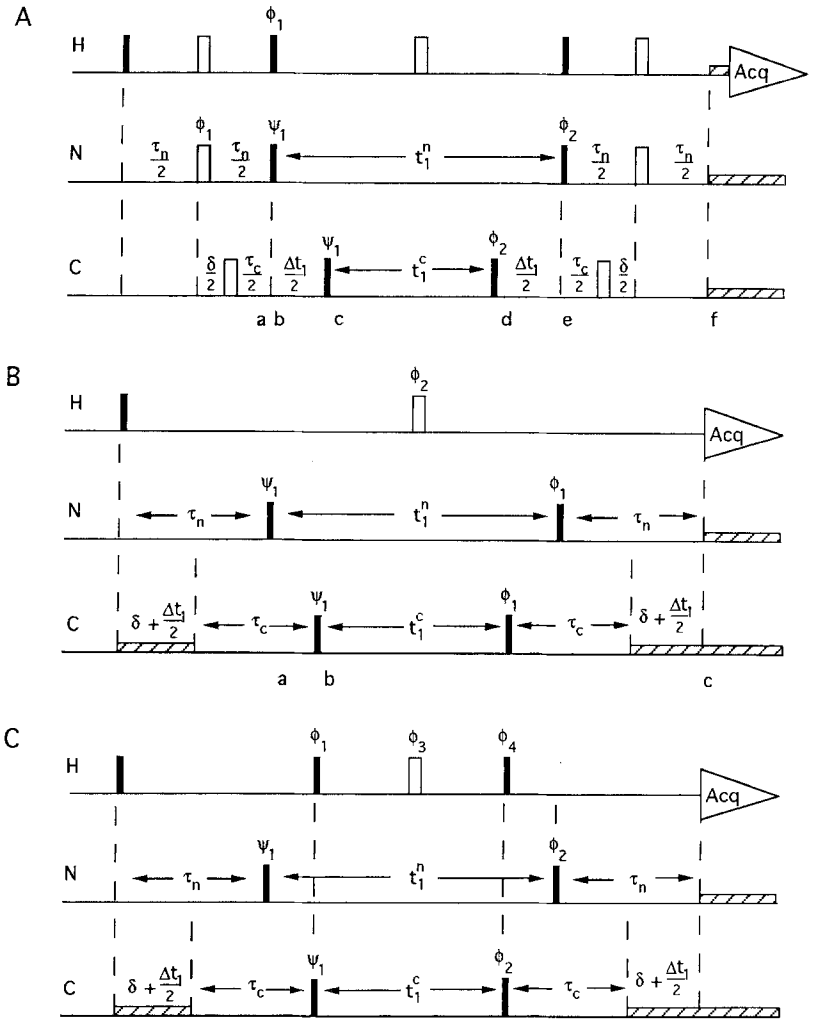

Fig. 1. Pulse schemes for the time-shared (TS) ($^{13}C/^{15}N$) heteronuclear correlation experiments. Shown are the sequences for (A) TS-HSQC; (B) TS-HMQC; (C) TS-HSMQC; and (D–F) pulsed field-gradient versions of these sequences. Narrow (filled) and wide pulses represent 90° and 180° pulses, respectively. The rectangles (dashed) indicate decoupling. Sine-bell-shaped gradient pulses (pfg) were given along the z-axis. Unless otherwise indicated, all pulses were applied along the x-axis. All sequences required moderate ^1H_2O presaturation. The TS-HSQC sequence (A) has the phase cycle ϕ_1 = y,−y; ϕ_2 = x,x,−x,−x; acq. = x,−x,−x,x. In all sequences ψ_1 = x. Quadrature detection in t_1 is obtained with States-TPPI, applied to ψ_1. The delays are defined as $\tau_n \approx 1/(2J_{NH})$ = 5 ms and $\tau_c \approx 1/(2J_{CH})$ = 3.4 ms, $\delta = \tau_n - \tau_c$ and t_1^n and t_1^c are the ^{15}N and ^{13}C evolution periods, respectively, and $\Delta t_1 = t_1^n - t_1^c$. The letters under the rf sequence are used in the text for a discussion of the magnetization flow. The phase cycle of the TS-HMQC sequence (B) was ϕ_1 = x,−x; ϕ_2 = x,x,−x,−x and acq. = x,−x. The phase cycle of the TS-HSMQC sequence (C) was ϕ_1 = x,y; ϕ_2 = x,x,−x,−x; ϕ_3 = x,y,x,y,−x,−y,−x,−y; ϕ_4 = −x,−y and acq. = x,−x,−x,x. The phase cycles for the gradient versions of the TS-HSQC (D) and TS-HMQC (E) were the same as those without gradients. The phase cycle of the gradient time-shared (GTS)-HSMQC sequence (F) was ϕ_1 = x,x,x,x,y,y,y,y; ϕ_2 = x,−x; ϕ_3 = x,x,−x,−x,y,y,−y,−y; ϕ_4 = −x,−x,−x,−x,−y,−y,−y,−y and acq. = x,−x,x,−x,−x,x,−x,x. In the sequences (B) and (C), for large values of Δt_1 the ^{13}C decoupling needs to be turned off after the first ^{15}N 90° pulse and turned on before the second ^{15}N 90° pulse, respectively. This can be accomplished on a Bruker AMX 600 (UXNMR

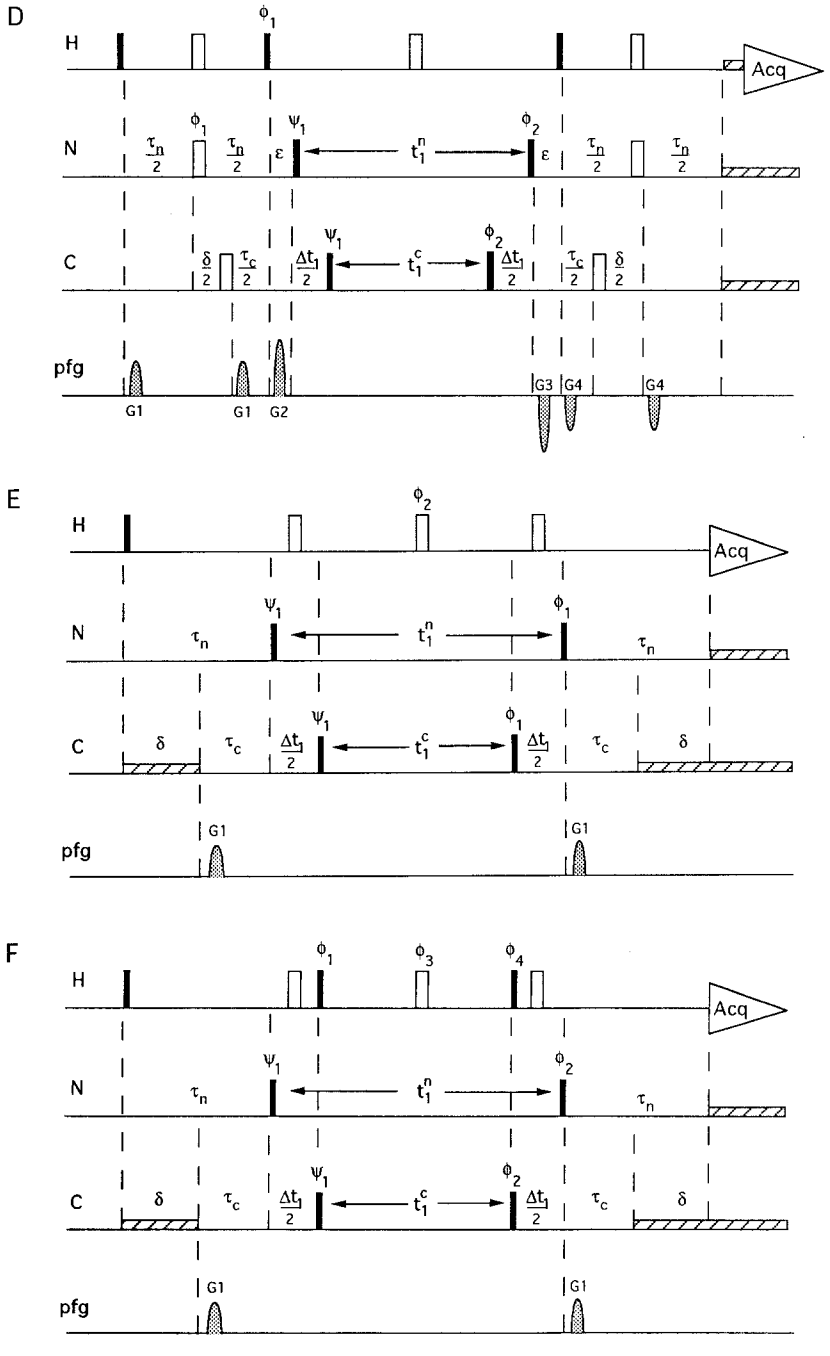

version 920801) by splitting the sequence in two different parts. The rf strengths were the following: for ^{1}H, γB_1 = 21 kHz; ^{1}H spin-lock, γB_1 = 10.5 kHz; $^{1}H_2O$ presaturation, γB_1 = 15 Hz (except D: γB_1 = 7.5 Hz); ^{15}N pulses, γB_1 = 9.6 kHz; ^{15}N decoupling (GARP), γB_1 = 1.1 kHz; ^{13}C pulses, γB_1 = 15.6 kHz; ^{13}C decoupling (GARP), γB_1 = 3.8 kHz. The gradient pulses all had a duration of 500 µs, followed by a 500-µs recovery delay; G_1 = −4 G/cm, G_2 = −12 G/cm, G_3 = 12 G/cm, G_4 = 4 G/cm.

is created. As described in Zuiderweg's paper (as well as below), the ratio of both types of coherences depends on the proton shift evolution in the period τ_n. By combining two experiments with different proton phase cycling, this chemical shift dependence and the associated phase-twisted lineshapes can be removed. The difference with the original sequence is that we decouple again for a period $\delta = (\tau_n - \tau_c)$, as in the TS-HMQC sequence, for optimal polarization transfer. Furthermore, the second ^{1}H 90° pulse is delayed with respect to the ^{15}N 90° pulse for the independent t_1^n and t_1^c evolution-time incrementation. Therefore, in the sequence of Fig. 1C the (^{15}N,^{1}H) coherences develop for a period ($t_1^n - t_1^c$) as pure multiple-quantum coherences and for a period t_1^c as mixed 'HSMQC' coherences. The pulse sequence of Fig. 1C shows that for protons the same number of 90° pulses is given as in the HSQC sequence of Fig. 1A, while for the heteronuclei the number of pulses equals that of the HMQC sequence of Fig. 1B. The small number of pulses applied to the heteronuclei is favourable and fewer artefacts than in the HSQC sequence can be expected. In addition, the longer relaxation time of the single-quantum contribution could lead to a better resolution than the HMQC sequence.

Figures 1D–F show the combination of these experiments with pulsed field-gradient methods for suppression of artefacts. The use of these gradients should not reduce the sensitivity of the heteronuclear correlation experiments. In Fig. 1D the TS-HSQC experiment was combined with gradients, as described by Bax and Pochapsky (1992) and Vuister et al. (1993) for traditional HSQC methods. The first two field-gradient pulses improve the three 180° refocussing pulses on ^{1}H, ^{13}C and ^{15}N, respectively. The third gradient pulse selects the H_zC_z and H_zN_z spin order of both heteronuclei. With the last three gradient pulses the opposite events occur. By use of these six gradient pulses the phase cycle of the TS-HSQC sequence can be reduced to two (with only ϕ_2 of Fig. 1A on the heteronuclei) or even be removed. Figure 1E shows a pulsed field-gradient version of the TS-HMQC sequence. In an HMQC experiment artefact suppression can be achieved by two gradient pulses, one in each delay for heteronuclear polarization transfer (Bax and Pochapsky, 1992). At long t_1-evolution periods we cannot use the TS-HMQC sequence of Fig. 1B directly in order to obtain independent spectral widths for ^{13}C and ^{15}N. Instead, we decouple the protons from carbon with two additional ^{1}H 180° pulses during the t_1^N evolution period. This will not affect the (^{15}N,^{1}H) multiple-quantum coherence and will still allow optimal polarization transfer for ^{13}C. In this way the total number of ^{13}C rf pulses remains the same as in the original HMQC sequences, while for protons the number of 180° pulses is the same as in an HSQC sequence. An alternative sequence using two additional 180° rf pulses on carbon instead of ^{13}C decoupling can, in principle, avoid the additional ^{1}H 180° rf pulses, but is expected to give poorer results, due to stronger relaxation of H_xC_z antiphase magnetization and due to weak rf strength towards the spectral borders of the ^{13}C dimension.

Finally, Fig. 1F shows the pulsed field-gradient version of the TS-HSMQC sequence. The sequence is very similar to the TS-HMQC sequence of Fig. 1E, except for two additional ^{1}H 90° rf pulses. It contains, however, an important advantage over the original HSMQC sequence. As pointed out, the HSMQC sequence creates a fraction of the magnetization as heteronuclear multiple-quantum coherence and another fraction as single-quantum coherence. As derived by Zuiderweg (1990), the detectable magnetization for ^{13}C-bound protons following the single-quantum route will be

$$(-H_y \cos^2 \omega_H \tau_c - H_x \cos \omega_H \tau_c \sin \omega_H \tau_c) \cos \omega_c t_1^c$$

and following the multiple-quantum route

$$(-H_y \sin^2 \omega_H \tau_c + H_x \cos \omega_H \tau_c \sin \omega_H \tau_c) \cos \omega_c t_1^c$$

The addition of both pathways leads to detectable magnetization $-H_y$, when both routes were equivalent. Since the T_2 relaxation rates of heteronuclear multiple-quantum and single-quantum coherences can be very different (Bax et al., 1990b; Seip et al., 1992), dispersive lineshape components (H_x) can develop, depending on the values of τ_c and ω_H. In order to remove the chemical-shift-dependent phase-twisted lineshapes, the HSMQC sequence requires an additional phase cycle on protons ($\phi_1 = y, \phi_3 = y, \phi_4 = -y$). By applying sufficiently strong field-gradient pulses in the delays for polarization transfer, however, the terms $\cos^2 \omega_H \tau_c$, $\sin^2 \omega_H \tau_c$ and $\cos \omega_H \tau_c \sin \omega_H \tau_c$ can be replaced by the averages $< \cos^2 \omega'_H \tau_c > = < \sin^2 \omega'_H \tau_c > = 0.5$ and $< \cos \omega'_H \tau_c \sin \omega'_H \tau_c > = 0$ with $\omega'_H = \omega_H + \gamma_c z G_z$, a positional-dependent ^1H resonance frequency. The use of the gradients removes the dispersive lineshape component H_x and thus the additional phase cycle can be removed. For the ^{15}N-bound magnetization the sequence of Fig. 1F leads to pure absorptive lineshapes as well, although the magnetization is only present during t_1^c as a mixture of multiple-quantum and single-quantum coherences and during the period Δt_1 as multiple-quantum coherence.

RESULTS AND DISCUSSION

In the above section we have described a series of time-shared experiments, that allow the simultaneous observation of the heteronuclear correlation spectra of two heteronuclei, in this case ^{13}C and ^{15}N. All proposed pulse sequences, i.e. TS-HSQC and its gradient version, TS-HMQC and TS-HSMQC (cf. Figs. 1A–D) have the same number of 'hard' pulses as the traditional sequences. Also, the gradient versions of TS-HMQC and TS-HSMQC (cf. Figs. 1E and F) do not have more ^1H pulses than a normal HSQC. In this respect these sequences should all have similar sensitivity. The differences with the traditional methods relate to a different use of delays and positioning of pulses and in some experiments to additional decoupling periods for one heteronucleus. All sequences can be combined with pulsed field-gradient techniques in a way similar to the traditional HMQC and HSQC pulse sequences (cf. Figs. 1D–F), leading to a reduction in phase cycles and to a suppression of artefacts. For HMQC and HSMQC this requires, however, two additional ^1H 180° pulses. All sequences allow an independent time incrementation of the ^{15}N and ^{13}C evolution periods t_1^n and t_1^c, which is required when the complete spectral widths for both nuclei need to be sampled. However, there is normally no ambiguity in the interpretation of multidimensional NMR spectra when the heteronuclear spectral domains are folded (Kay et al., 1989; Bax et al., 1991). When the ^{13}C spectral domain is folded several times and the ^{15}N domain once, the spectral widths for both nuclei can be adjusted to very similar values. In that case the time-sharing methods will hardly involve a compromise. As pointed out above, the proposed sequences need short phase cycles (certainly when combined with pulsed field gradients), making them suitable for use in heteronuclear multidimensional NMR.

The pulse sequences of Fig. 1 have been tested with a (^{13}C,^{15}N) uniformly enriched HU protein. The histone-like HU protein from *Bacillus stearothermophilus* is a dimeric protein with a molecular weight of 18 kDa, each monomer consisting of 90 residues (Tanaka et al., 1984). Figures 2A

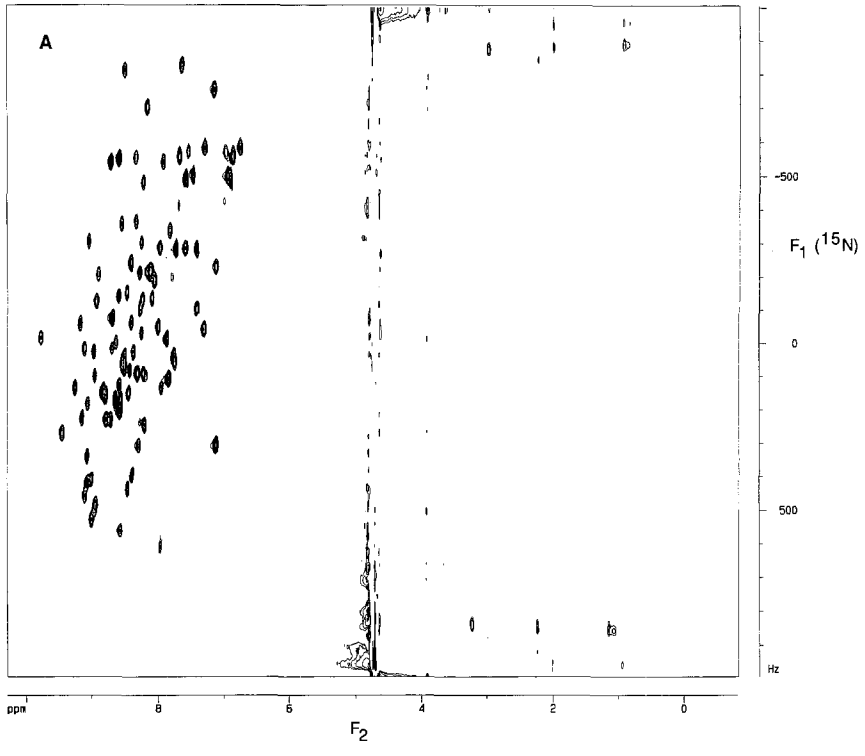
A
-500
F1 (15N)
0
500
Hz
ppm
8
6
4
2
0
F2

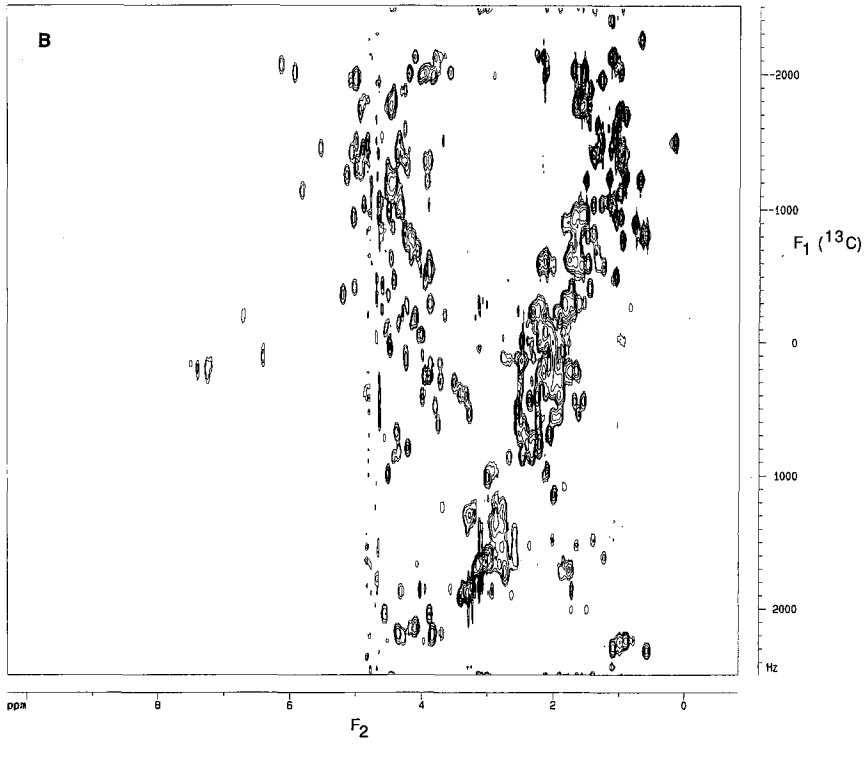
B
-2000
-1000
F1 (13C)
0
1000
2000
Hz
ppm
8
6
4
2
0
F2

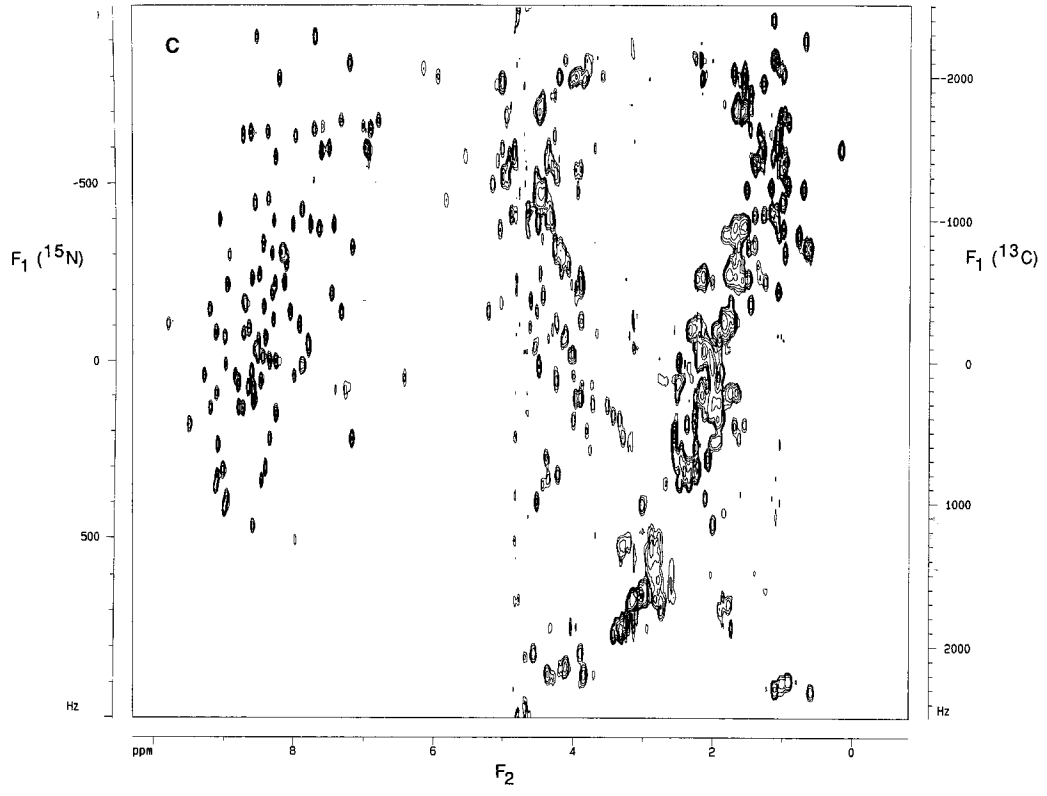

Fig. 2. (A) Regular (^{15}N,^{1}H) HSQC, (B) regular (^{13}C,^{1}H) HSQC, and (C) time-shared (TS) ($^{15}N/^{13}C$,^{1}H) HSQC spectra of fully (^{13}C,^{15}N)-enriched HU protein in H_2O. The spectra of (A) and (B) were recorded using the pulse sequence and phase cycles as described by Bax et al. (1990b). The TS-HSQC spectrum (C) was recorded using the pulse sequence of Fig. 1A. The delays and pulse strengths were the same as described in Fig. 1. The HU protein was dissolved in 95% $^{1}H_2O$/5% $^{2}H_2O$, pH = 4.6, 200 mM KCl. The spectra were recorded on a standard Bruker AMX 600 spectrometer, equipped with a shielded-gradient (^{13}C,^{15}N) triple-resonance probehead and using a field-gradient accessory with a 10-A amplifier. The ^{13}C rf pulses were given with a linear 300 W rf amplifier. The t_1 increment for ^{15}N was 500 μs and for ^{13}C 200 μs, leading to spectral widths of 2000 and 5000 Hz, respectively. For the TS-HSQC spectrum the t_1 increment for ^{13}C was 200 μs and with Δt_1 = 300 μs for ^{15}N, a net t_1 increment of 500 μs was created, leading to the same spectral widths for ^{15}N and ^{13}C as in (A) and (B), respectively. The ^{15}N rf frequency in (C) was chosen 100 Hz higher than in (A) in order to avoid overlap. The spectra were recorded using the States-TPPI method for quadrature detection in the f_1 dimension. The initial t_1-values were set in such a way that first-order phase corrections of 360° resulted and that folded signals would appear at positive levels. The number of scans was 8 and the sizes of the recorded data sets were 64* (t_1) × 1024* (t_2), where n* are complex points. The data were apodized by a 72° shifted sine-bell window in t_1 and a 90° shifted squared sine-bell window in t_2.

and B show the regular (^{15}N,^{1}H) and (^{13}C,^{1}H) HSQC spectra of this protein. The ^{13}C frequencies of the (^{13}C,^{1}H) HSQC spectrum were folded several times as would be done normally for 3D and 4D NMR spectroscopy. By overlaying the spectra, it is apparent that in time-shared experiments overlap of the 2D cross peaks can be avoided by a suitable choice of the ^{15}N and ^{13}C spectral frequencies and spectral widths. Figure 2C shows the TS- ($^{13}C/^{15}N$,^{1}H) HSQC spectrum of the HU protein. For the ^{15}N and ^{13}C dimensions, spectral widths of 2000 and 5000 Hz respectively were chosen. The comparison with the spectra of Figs. 2A and B shows, that the combination technique results in spectra of similar sensitivity to that obtained in the separate recordings. Loss

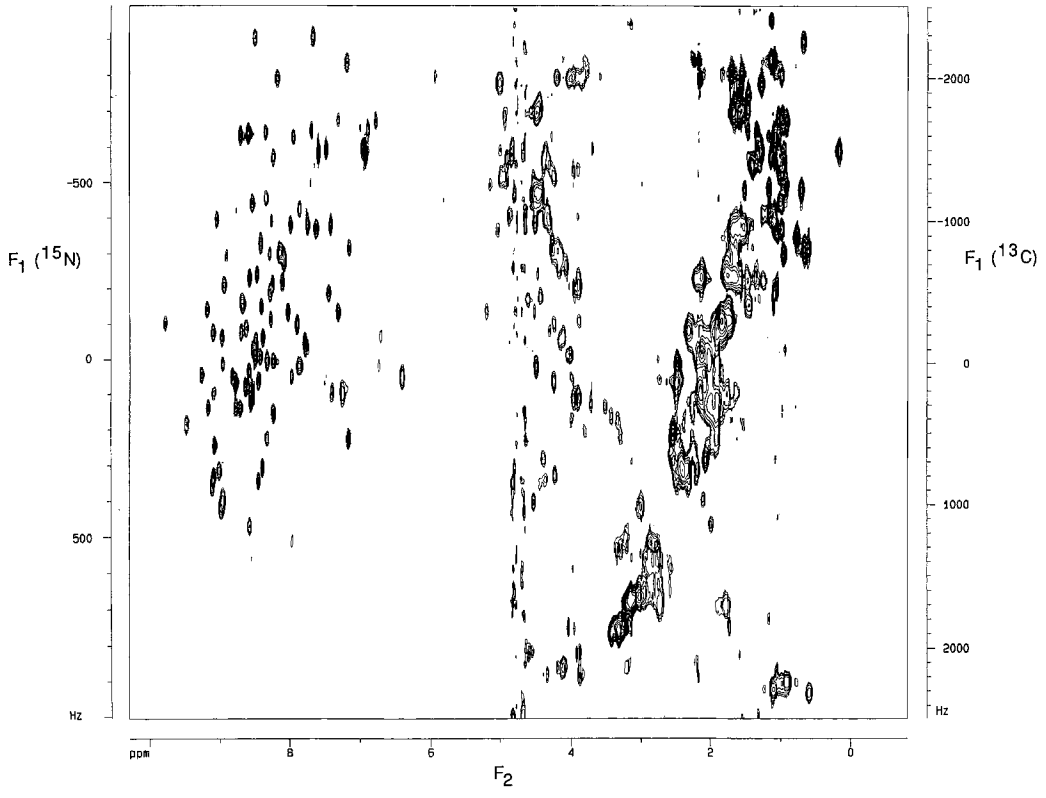

Fig. 3. Gradient-time-shared (GTS)-HSMQC spectrum of fully (^{13}C,^{15}N)-enriched HU protein in H_2O. The spectrum was recorded with the sequence of Fig. 1F. In this case the number of scans was only 2. Further conditions are similar to those of Fig. 2.

in sensitivity for ^{13}C in the pulse scheme of Fig. 1A may be expected in the time period 2δ by relaxation of H_x and H_y carbon-attached proton magnetization and of H_xC_z and H_yC_z antiphase magnetization, and in the incrementing period ($t_1^n - t_1^c$) by relaxation of H_zC_z spin order. With the values chosen (2δ = 3.2 ms and $(t_1^n - t_1^c)^{max}$ = 19.2 ms), we observed a loss of maximally 20% on most ^{13}C cross peaks, comparing the HSQC spectra of Figs. 2A and B with that of Fig. 2C. Such a loss would still be acceptable for most multidimensional spectra, where digital resolution is more often the issue. A potential danger of the HSQC sequence of Fig. 1A, at least when combined with the independent incrementation of the ^{13}C and ^{15}N spectral widths, could be imperfect ^{13}C 180° pulses. During the ($t_1^n - t_1^c$) periods C_y magnetization terms might evolve, which cannot be phase-cycled out by short phase cycles as would be required for multidimensional spectra. A remedy would be to use pulsed field gradients as in the sequence of Fig. 1D. In our spectra no such artefacts were observed, however. For ^{15}N no artefacts or loss in sensitivity is expected and this is what is indeed observed.

For the HU protein the pulse sequence for the time-shared ($^{13}C/^{15}N$,^1H) HMQC (Fig. 1B) gives a spectral quality that is very similar to the regular HMQC spectra with ^{15}N and ^{13}C separately (data not shown). Compared to the HSQC spectra of Fig. 2, it shows additional line broadening, due to a large extent to unresolved J_{HH} coupling (Bax et al., 1990b). Artefacts due to imperfect ^{13}C

or ^{15}N pulse lengths are not expected in the sequence of Fig. 1B, since we chose to compensate the difference in heteronuclear $^1J_{HX}$ values by decoupling ^{13}C over the period $\delta = \tau_n - \tau_c$, rather than by using ^{13}C 180° pulses. Such artefacts were indeed not observed. For the ^{13}C part of the combined HMQC sequence sensitivity loss is expected in the incrementing delay $2\delta + (t_1^n - t_1^c)$ by relaxation of H_y and H_x magnetization terms for protons attached to ^{13}C. In our experiments this delay ran from 3.2 to 22.4 ms, leading to an observed peak sensitivity loss of 20–50% for nitrogen and carbon as compared to the HSQC spectra of Fig. 2. It should be noted, however, that the large loss for the (^{15}N,^1H) and ($^{13}C^\alpha$,$^1H^\alpha$) cross peaks is partly due to the HMQC method itself and not related to the time-shared technique. Despite the lower signal-to-noise ratio of the simultaneous HMQC method for the HU protein, the sequence of Fig. 1B may still have significant advantages when combined with multidimensional techniques, since it requires a minimal phase cycling of only two steps for artefact suppression and since shorter evolution periods will be used in these cases.

Recently, it was pointed out that a higher sensitivity than in the HMQC sequence could be obtained by a combined HMQC/HSQC method (Zuiderweg, 1990). An advantage of the time-shared ($^{13}C/^{15}N$,^1H) HSMQC experiment shown in Fig. 1C is that it contains no heteronuclear 180° pulses, so that artefacts due to imperfect heteronuclear pulse lengths should not arise. For the HU protein the observed sensitivity is indeed considerably higher than in a TS-HMQC spectrum, especially for the (C^α,H^α) coherences, being more similar to the TS-HSQC sequence of Fig. 2C (data not shown). However, the required minimal phase cycle for an HSMQC spectrum has a length of four, as compared to two for an HMQC sequence, which could be too long for application in multidimensional NMR. As pointed out above, the phase cycle of the HSMQC sequence can be reduced by use of field gradients. Figure 3 shows an example of the pulsed field gradient TS-HSMQC spectrum of the HU protein, recorded with a phase cycle of only two steps. The spectrum was of a quality similar to that of the TS-HSMQC experiment without gradients (data not shown). This demonstrates that for HSMQC, the phase cycling can indeed be reduced. The lower sensitivity in the spectrum of Fig. 3 compared to Fig. 2C is mainly due to the lower number of scans.

Of course, the proposed pulse sequences also have drawbacks, as compared to recording the separate spectra. For ^{13}C, loss in sensitivity is anticipated due to the additional delays. When the time-shared experiment should focus on ^{13}C, one could choose a shorter delay for ^{15}N polarization transfer, τ_n. This will reduce relaxation losses for the (^{13}C,^1H) coherences, but at the expense of the (^{15}N,^1H) cross-peak intensities. Furthermore, the ^{13}C decoupling time is longer than in the traditional sequences and there is the problem, already mentioned above, of imperfect 180° pulses in the HSQC sequence, possibly leading to spectral artefacts. In this last aspect the proposed HMQC and HSMQC sequences will be more robust, but for long t_1 acquisition times they give rise to broader resonances in the ω_1 domain, mainly due to unresolved J_{HH} coupling (Bax et al., 1990b). Additional anticipated problems of the proposed sequences (at least for fully enriched proteins) could be signal broadening due to unresolved J_{CN} and J_{CC} couplings. For J_{CN} these effects seem less important, at least when the acquisition times are shorter than $1/2J_{CN}$. For J_{CC} an improvement in resolution can be obtained by CO decoupling and by implementing constant-time methods (Vuister and Bax, 1992). For ^{15}N a possible drawback is that during the acquisition there is simultaneous decoupling for ^{15}N and ^{13}C, which will naturally cause more sample heating. We also noted that the simultaneous ^{15}N and ^{13}C decoupling through close cables to our

(^{13}C,^{15}N,^{1}H) triple-resonance probehead can create a signal at a ($^{13}C - ^{15}N$) difference frequency, which interferes with the ^{2}H lock regulation. By use of band-selective filters, by leading the cables from the amplifiers separately and directly to the probehead and by use of well-shielded ^{2}H lock cables such problems can be minimized.

At the moment it is difficult to give a preference for TS-HSQC, TS-HMQC or TS-HSMQC. By recording spectra with the various sequences of Fig. 1, it became apparent that the choice between TS-HMQC and TS-HSMQC depends largely on the length of the t_1 acquisition times. For 4D NMR, where the acquisition periods are generally short, HMQC should be preferred since there are fewer pulses. The HSQC sequence gave good sensitivity and the narrowest signals for ^{15}N, but the high resolution is only obtainable in case of long sampling times for the heteronucleus, which will not be the case in 3D and 4D NMR. The HSQC sequence has more heteronuclear pulses than the other two, leading to more potential artefacts (which can be overcome by pulsed field gradients) and loss in sensitivity, especially for ^{13}C. The HMQC sequence has a clear advantage, since it requires only a minimal phase cycle of two steps, but its resolution and sensitivity for ^{15}N were relatively low. The HSMQC sequence was intermediate in sensitivity, but definitely required a minimal phase cycle of four when used without gradients. As shown, many of the mentioned drawbacks can easily be overcome when these sequences are combined with pulsed field-gradient methods. Under the conditions of Fig. 3, the gradient time-shared (GTS) HMQC and GTS-HSMQC techniques for the HU protein resulted in a 25–30% higher intensity than a TS-HSQC method for many (^{13}C,^{1}H) cross peaks, but in a 30–40% lower intensity for many (^{15}N,^{1}H) cross peaks. When the principal aim is the observation of ^{13}C-attached protons, the TS-HMQC sequence will be the method of choice. The TS-HSQC sequence performs best if the focus is on ^{15}N-attached protons. Therefore, GTS-HSMQC could be a good compromise.

CONCLUSIONS

We have described several new methods for the simultaneous acquisition of heteronuclear 2D spectra of different nuclei. The methods are particularly suited for the simultaneous observation of (^{15}N,^{1}H) and (^{13}C,^{1}H) coherences in (^{13}C,^{15}N) uniformly enriched proteins, where they could be applied for reducing measuring times or improving spectral resolution of multidimensional NMR spectra. For this purpose, the phase cycles of the HMQC, HSQC and HSMQC pulse sequences were designed for the simultaneous observation of the (^{13}C,^{1}H) and (^{15}N,^{1}H) coherences. In most cases overlap of both kinds of coherences can be avoided in 2D spectra, by using the difference in chemical shift (for the aliphatic and amino protons) and by selecting suitable ^{15}N and ^{13}C spectral widths and spectral frequencies (for the aromatic and amino protons). However, with larger phase-cycling schemes independent heteronuclear filtering for (^{13}C,^{1}H) and (^{15}N,^{1}H) coherences is also possible, since the separate 2D (^{13}C,^{1}H) and (^{15}N,^{1}H) spectra can be obtained by linear combination of two data sets, as was pointed out by Sørensen (1990) and Farmer (1991). The latter method seems most useful for applications of the combination technique where a large number of scans is required, such as for heteronuclear relaxation measurements and measurements at natural abundance. In this case the time saving can be translated into a higher signal-to-noise ratio, given a fixed measuring time. However, the major application of the proposed time-shared technique seems the use as a building block in heteronuclear 3D and 4D NMR measurements of (^{13}C,^{15}N) fully enriched proteins, which are currently being developed in our

laboratory. In that case the time-shared method has the principal advantage over the traditional sequences that it allows the simultaneous observation of all protons in one data set.

ACKNOWLEDGEMENTS

We thank Dr. C.E. Vorgias and Dr. K.S. Wilson (EMBL, Hamburg) for providing the (^{13}C,^{15}N) fully enriched HU protein sample. This research was supported by the Netherlands Foundation for Chemical Research (SON) with the aid of the Netherlands Organisation of Scientific Research (NWO).

REFERENCES

Bax, A., Griffey, R.H. and Hawkins, B.L. (1983) *J. Magn. Reson.*, **55**, 301–315.
Bax, A., Clore, G.M., Driscoll, P.C., Gronenborn, A.M., Ikura, M. and Kay, L.E. (1990a) *J. Magn. Reson.*, **87**, 620–627.
Bax, A., Ikura, M., Kay, L.E., Torchia, D.E. and Tschudin, R. (1990b) *J. Magn. Reson.*, **86**, 304–318.
Bax, A., Ikura, M., Kay, L.E. and Zhu, G. (1991) *J. Magn. Reson.*, **91**, 174–178.
Bax, A. and Pochapsky, S. (1992) *J. Magn. Reson.*, **99**, 638–643.
Bax, A. and Grzesiek, S. (1993) *Acc. Chem. Res.*, **26**, 131–138.
Bendall, M.R., Peggy, D.T. and Doddrell, D.M. (1983) *J. Magn. Reson.*, **52**, 81–117.
Bodenhausen, G. and Ruben, D.J. (1986) *Chem. Phys. Lett.*, **69**, 185–189.
Clore, G.M. and Gronenborn, A.M. (1991) *Prog. NMR Spectrosc.*, **23**, 43–92.
Clore, G.M., Kay, L.E., Bax, A. and Gronenborn, A.M. (1991) *Biochemistry*, **30**, 12–18.
Davis, A.D., Boelens, R. and Kaptein, R. (1992) *J. Biomol. NMR*, **2**, 395–400.
Ernst, R.R., Bodenhausen, G. and Wokaun, A. (1987) *Principles of Nuclear Magnetic Resonance in One and Two Dimensions*, Clarendon Press, Oxford.
Farmer II, B.T. (1991) *J. Magn. Reson.*, **93**, 635–641.
Hurd, R.E. (1990) *J. Magn. Reson.*, **87**, 422–428.
Ikura, M., Kay, L.E. and Bax, A. (1990a) *Biochemistry*, **29**, 4654–4667.
Ikura, M., Kay, L.E., Tschudin, R. and Bax, A. (1990b) *J. Magn. Reson.*, **86**, 204–209.
Kay, L.E., Marion, D. and Bax, A. (1989) *J. Magn. Reson.*, **84**, 72–84.
Kay, L.E., Clore, G.M., Bax, A. and Gronenborn, A.M. (1990) *Science*, **249**, 411–414.
Keeler, J., Davis, A.L. and Laue, E.D. (1993) *Methods Enzymol.*, in press.
Marion, D., Kay, L.E., Sparks, S.W., Torchia, D.A. and Bax, A. (1989) *J. Am. Chem. Soc.*, **111**, 1515–1517.
Müller, L. (1979) *J. Am. Chem. Soc.*, **101**, 4481–4484.
Seip, S., Balbach, J. and Kessler, H. (1992) *J. Magn. Reson.*, **100**, 406–410.
Sørensen, O.W. (1990) *J. Magn. Reson.*, **89**, 210–216.
Tanaka, I., Appelt, K., Dijk, J., White, S.W. and Wilson, K.S. (1984) *Nature*, **310**, 376–381.
Vuister, G.W., Boelens, R., Kaptein, R., Hurd, R.E., John, B. and Van Zijl, P.C.M. (1991) *J. Am. Chem. Soc.*, **113**, 9688–9690.
Vuister, G.W. and Bax, A. (1992) *J. Magn. Reson.*, **98**, 425–433.
Vuister, G.W., Clore, G.M., Gronenborn, A.M., Powers, R., Garrett, D.S., Tschudin, R. and Bax, A. (1993) *J. Magn. Reson. Ser. B*, **101**, 210–213.
Zuiderweg, E.R.P. and Fesik, S.W. (1989) *Biochemistry*, **27**, 3568–3580.
Zuiderweg, E.R.P. (1990) *J. Magn. Reson.*, **86**, 314–318.
Zuiderweg, E.R.P., McIntosh, L.P., Dahlquist, F.W. and Fesik, S.W. (1990) *J. Magn. Reson.*, **86**, 210–216.
Zuiderweg, E.R.P., Petros, A.M., Fesik, S.W. and Olejniczak, E.T. (1991) *J. Am. Chem. Soc.*, **113**, 370–372.